

# Lyman- $\alpha$ emitters with red colors at $z \simeq 2.4$

Massimo Stiavelli<sup>1</sup>, Claudia Scarlata<sup>2</sup>

Space Telescope Science Institute, 3700 San Martin Dr., 21218 MD, U.S.A.; mstiavel@stsci.edu,  
scarlata@stsci.edu

Nino Panagia<sup>3</sup>

Space Telescope Science Institute, 3700 San Martin Dr., 21218 MD, U.S.A.; panagia@stsci.edu

Tommaso Treu

California Institute of Technology, MS 105-24, Pasadena, CA 91125, U.S.A.; tt@astro.caltech.edu

Giuseppe Bertin

Università degli Studi di Milano, via Celoria 16, I20133 Milano, Italy; Giuseppe.Bertin@mi.infn.it

Francesco Bertola

Università degli Studi di Padova, vicolo dell'Osservatorio 5, I35122, Padova, Italy;  
bertola@pd.astro.it

## ABSTRACT

We have carried out a search for Lyman- $\alpha$  emission from galaxies at  $z \simeq 2.4$  over a field of  $1200 \text{ } \square'$  using the CFH12K camera at the CFHT and a custom medium band filter. The search has uncovered 58 candidates, corresponding to a completeness-corrected source density of  $\sim 0.07 \text{ } \square'^{-1}$ . Our sources have red colors ( $\overline{B-I} \simeq 1.8$ ) which imply either that a large fraction of the light is highly reddened and we are detecting Lyman- $\alpha$  through special lines of sight, or that these objects contain an underlying older stellar population. While for each individual object we cannot discriminate between these alternatives, we conclude that most of the objects actually contain an older component because the star formation rates inferred from the picture based on reddening, applied to all candidates, would imply an exceedingly high star formation rate, *i.e.* more than two orders of magnitude above the peak cosmic star formation rate (e.g. Lilly et al. 1996).

*Subject headings:* galaxies: elliptical and lenticular, cD — evolution — formation —;  
cosmology: observations; infrared: galaxies

---

<sup>1</sup>Visiting Astronomer, Canada-France-Hawaii Telescope, which is operated by the National Research Council of Canada, the Centre Nationale de la Recherche Scientifique of France, and the University of Hawaii

<sup>2</sup>also Università degli Studi di Padova, Italy

<sup>3</sup>On assignment from the Space Science Dept. of ESA

## 1. Introduction

In recent years, the study of the global star formation rate of the Universe has become a very popular subject after it was introduced and developed as a diagnostic technique by a number of seminal papers (Pei & Fall 1995, Lilly et al. 1996, Madau et al. 1996.) Several authors have noted some limitations of the original approach based on the HDFN data (Madau et al. 1996) especially for two reasons:

- i)* Estimating the star formation rate (hereafter SFR) from the UV flux might underestimate the true SFR because of the effects of dust extinction (Meurer, Heckman, & Calzetti 1999, Calzetti & Heckman 1999, Pei et al. 1999)
- ii)* The small area of the HDF may suffer from cosmic variance, especially because the brightest, relatively rare, sources may be seriously affected by small number statistics and clustering (Steidel et al. 1996, Steidel et al. 1998).

Even disregarding these limitations, the cosmic star formation history provides only partial information about how individual galaxies evolve. A low mean metallicity of the Universe at some redshift might imply either that all galaxies were in place and metal poor at that redshift or that only a few, possibly metal rich, galaxies had formed early on. Indeed, evidence for the latter interpretation may be found in the scatter in metallicity of damped Lyman- $\alpha$  systems and in the relatively high metallicity of the  $z = 0.5 - 1$  CFRS galaxies (Carollo & Lilly 2001).

A clear answer to these questions could be found by simultaneously measuring star formation rate, metallicity, and dust content for a statistically significant sample of high redshift ( $z \geq 2$ ) galaxies. A reliable measurement of the gas physical properties requires access to the rest frame optical spectrum and in particular to the Balmer lines, and to the [NII] $\lambda\lambda 6548, 6583$ , [OIII] $\lambda\lambda 4959, 5007$  and [OII] $\lambda\lambda 3727, 3729$  doublets (e.g., Kennicutt 1998; Stiavelli 1998). This has been attempted only for a handful of objects (Kobulnicky & Koo 2000, see also Moorwood et al. 2000, Pettini et al. 2001). The  $z \simeq 2.4$  redshift window is ideal for this kind of measurements since at this redshift all of these lines fall in the Near-IR atmospheric windows. At the same time  $z \simeq 2.4$  is larger than that of the peak in the global star formation rate as claimed by Madau et al. (1996). For this reason, we have started a search for Lyman- $\alpha$  emitters with the CFH12K camera at the CFHT using a custom medium band filter centered at 4158 Å. The area covered is 1200  $\square'$ . The survey is briefly described in Section 2. Our sample of bona fide Lyman- $\alpha$  emitters is described and discussed in Section 3. Section 4 contains our general discussion and conclusions.

## 2. The survey

The CFH12K camera at the CFHT is a mosaic of 12 MIT Lincoln Lab CCDs each 2K by 4K pixels. The pixel size is 0.2", yielding a total field of view of 42 by 30  $\square'$ . We carried out our observations in July 27-August 1, 2000. The main filter used was a custom medium band

interference filter with central wavelength 4158 Å and width 174 Å aimed at detecting Lyman- $\alpha$  at  $z=2.422\pm0.072$ . The filter peak throughput is 65 %. We obtained images for a total exposure time of 19,800s on a field offset by  $\sim 120$  arcsec from the QSO DMS 2139-0356 at  $z \simeq 2.36$ . For the same field, we also obtained exposures for 3000s in I band and 6600s in B band. After standard reduction steps, the images were combined using a standard CR-rejection algorithm (IRAF's *imcombine*). The photometric calibration was based on the nominal zero-points for the camera and checked by observing standard stars in the Landolt field SA 107 (Landolt 1992). All magnitudes and fluxes were also corrected for galactic extinction ( $E(B-V) = 0.055$ ). A more detailed description of the data reduction and analysis is presented separately (Scarlata et al. 2001).

Once the images were reduced and combined, they were searched for objects using the SExtractor package (Bertin & Arnouts 1996). We verified our object finding algorithm by comparing the B band number counts with those of Metcalfe et al. (2001) and found good agreement down to  $B \simeq 25$ . The photometric accuracy of our procedure was tested extensively by introducing artificial stars on our images and recovering them. The same simulations provided us also with the completeness correction as a function of flux.

Continuum subtraction was carried out by deriving the histogram of Lyman- $\alpha$  to B band flux ratios for all sources in each chip (excluding saturated stars). From the histogram we derived the median flux ratio and the FWHM of the histogram which we use as a measure of the intrinsic cosmic dispersion in the ratio. Our selection criterion requires the line excess to be both statistically significant and larger than the cosmic dispersion. A source was considered a candidate if the flux in the Lyman- $\alpha$  medium band exceeded both: *i*) the continuum contribution - estimated with the Lyman- $\alpha$  over continuum ratio - by more than  $3\sigma$  and *ii*) the value corresponding to the ratio plus one histogram FWHM. The exclusion of sources with ratios within one histogram FWHM eliminates high S/N sources within the cosmic scatter. The validity of this procedure was checked by estimating the expected continuum contribution in the Lyman- $\alpha$  medium band filter by using spectral synthesis models (Bruzual & Charlot 1993). For the selection of our sample, we adopted the observed ratio rather than the theoretical values because the former is robust with respect to uncertainties in the filter effective wavelengths and in the exact QE shape of the various CCDs and calibration uncertainties. Our results do not critically depend on this choice. Our  $3\sigma$  line flux limit for a source without continuum is  $\sim 2 \times 10^{-16}$  erg s $^{-1}$  cm $^{-2}$ . A total of 89 sources were found with significant emission in the medium band filter. No overdensity was found associated with the QSO DMS 2139-0356.

The most serious contamination of our sample is expected to be due to [OII] $\lambda\lambda 3726, 3729$  emitters at  $z \simeq 0.11$ . In order to remove this contamination we considered the distribution of local [OII] emitters (Jansen et al. 2000) in the equivalent width (EW)- $M_B$ -(B-R) space and compared it to our sources (Figure 1). We assumed that they were *all* located at  $z \simeq 0.11$  and compared their properties with those of the local [OII] emitters (moved to  $z=0.11$ ). The B-R colors of our sources were obtained from the measured B-I by applying a K-correction for  $z \simeq 0.11$  derived

from galaxy templates and spectral synthesis models. The comparison shows that the local [OII] emitters are on average brighter than our candidates. This may be partly due to the magnitude limit of the local sample but is also due to the fact that our sources would be very faint (and very compact) if at low redshift. In addition, the local emitters show trends of increasing EW with decreasing luminosity (top left panel in Figure 1), increasing EW with bluer colors (top right panel), and bluer colors with decreasing luminosity (bottom left panel). We determined best fits to these relations and produced a delta-delta plot by subtracting from the Log EW and B-R color of each object the mean value corresponding to its absolute magnitude. In the delta-delta plot we thus identify the bona fide Lyman- $\alpha$  emitters as those objects that lie outside the locus of the local [OII] objects. Such an approach is pessimistic since it assumes that all those objects that are along the mean relations observed for [OII] emitters at low redshift are indeed such. A total of 31 sources are thus rejected. We should note that the Jansen et al. (2000) sample is a fair representation of local galaxies only down to absolute magnitude  $M_B = -14$ . One might imagine a population of fainter starbursting dwarfs with intrinsically much higher [OII] EW contaminating our sample of bona fide candidates. We think that this is highly unlikely since: *i*) all local group dwarfs fainter than  $M_B = -14$  have little or no line emission, *ii*) even local starburst and blue compact galaxies (see, e.g., McQuade, Calzetti & Kinney 1995) do not show [OII] EW in excess of 100. Thus, we will assume the validity of our rejection and base our analysis on the remaining 58 objects, implying a density of  $0.07 \pm 0.01$  sources  $\square'^{-1}$  above  $2 \times 10^{-16}$  erg cm $^{-2}$  s $^{-1}$ . This density estimate has been corrected for completeness and (statistically) for the number ( $\sim 6$ ) of  $3\text{-}\sigma$  sources expected to be due to random fluctuations. Our sample contains 6 candidates at  $5\text{-}\sigma$  and 9 at  $4\text{-}\sigma$ .

Our confidence about the robustness of the sample of bona fide Lyman- $\alpha$  emitters is reinforced by a comparison with other authors. Steidel et al. (2000) focus on a known overdensity at  $z \simeq 3.09$ , with a fainter flux limit and a narrower filter. They find a density of 0.9 sources  $\square'^{-1}$ . Once this density is reduced by a factor 6 to allow for their estimate of the field overdensity, we derive a density of 0.16 sources  $\square'^{-1}$  which compares favourably with our value of 0.07 sources  $\square'^{-1}$ . Out of 77 candidates selected from the excess emission in the narrow band filter, Steidel et al. (2000) identify 5 as contaminants, i.e., a fraction of 6.4 %. For our sample we have a more conservative fraction of interlopers of 35 %. This level of agreement is comforting given the differences between the two samples. Searching on a known overdensity, Campos et al. (1999) had a flux limit of  $6 \times 10^{-17}$  erg cm $^{-2}$  s $^{-1}$  and  $\Delta z \simeq 0.1$ . They found a surface density of objects of about 0.33  $\square'^{-1}$  at  $z \simeq 2.5$  which is not incompatible with our result. Other searches (De Propris et al. 1993; Thompson et al. 1995) sampled smaller areas at shallower limits so that our results remain compatible with their upper limits.

### 3. The sample

The total Lyman- $\alpha$  emission from our sample is  $2.1 \times 10^{-14}$  erg cm $^{-2}$  s $^{-1}$  which increases to  $(3.1 \pm 0.4) \times 10^{-14}$  erg cm $^{-2}$  s $^{-1}$  when corrected for completeness. The star formation rate can

be estimated directly from the Lyman- $\alpha$  flux following Charlot & Fall (1993). In the absence of attenuation and adopting  $H_0=65 \text{ km s}^{-1} \text{ Mpc}^{-1}$ , we find a star formation rate per unit volume of  $0.008 \text{ M}_\odot \text{ yr}^{-1} \text{ Mpc}^{-3}$  for  $\Omega = 1$  or  $0.005 \text{ M}_\odot \text{ yr}^{-1} \text{ Mpc}^{-3}$  for  $\Omega_M = 0.3 \Omega_\Lambda = 0.7$ . These values are accurate to within a factor of 2. By comparing the measured value of the EW to the theoretical prediction one obtains a direct measure of the resonant attenuation of Lyman- $\alpha$ . Our sources have  $\overline{\text{EW}} \simeq 39$ , implying an attenuation correction of  $\sim 3.8$ . The corrected star formation rates per unit volume is  $0.03 \text{ M}_\odot \text{ yr}^{-1} \text{ Mpc}^{-3}$  for  $\Omega = 1$  or  $0.02 \text{ M}_\odot \text{ yr}^{-1} \text{ Mpc}^{-3}$  for  $\Omega_M = 0.3 \Omega_\Lambda = 0.7$ . These values are  $\sim 17\%$  of the value determined by Madau et al. (1996) for  $z \simeq 2.75$  and 5% of the Lilly et al. (1996) peak at  $z=1$ .

A more empirical estimate can be obtained by adopting case B recombination theory and the calibration by Kennicutt, Tamblyn, & Congdon (1994). This would yield about 15 % of the value determined by Madau et al. (1996) for  $z \simeq 2.75$  and 4% of the Lilly et al. (1996) peak at  $z=1$ . Higher values would be estimated by following Giavalisco, Koratkar, & Calzetti (1996) and adopting an average Lyman- $\alpha$  attenuation by a factor  $\sim 10$ .

An independent estimate of the SFR for our sample can be made on the basis of their rest frame UV flux as derived from the B band magnitudes. This will be uncertain to about a factor two because our B filter includes also wavelengths beyond Lyman- $\alpha$  where absorption by the Lyman- $\alpha$  forest can play a role. The same calibration as in Madau et al. (1996) gives a star formation rate  $\sim 18\%$  of the  $z = 2.75$  value, in good agreement with the estimate based on the Lyman- $\alpha$  emission.

In Figure 2 we plot the EW vs the measured B-I color for our sample (filled circles). The symbol size identifies objects detected at 5 (largest), 4 (intermediate), and 3- $\sigma$  (smallest). For reference we plot as open circles the points that are considered as possible low redshift contaminants ([OII] emitters). The dotted and dashed lines give the relation between EW and B-I color derived on the basis of Bruzual & Charlot (1993, BC96) models for constant star formation and single bursts, respectively. The model spectra were corrected for the intergalactic attenuation due to neutral hydrogen along the line of sight following the prescriptions by Madau (1995). Clearly the red colors of our sources are compatible with those observed by Pascarelle et al. (1998) in a field centered on a known overdensity at  $z \simeq 2.4$  (open triangles) and in three random WFPC2 fields (open stars). The observed colors and Lyman- $\alpha$  EWs are incompatible with those of simple stellar population models. This was noted also by Campos et al. (1999) for their sample. A couple of Lyman- $\alpha$  emitting objects with very red colors have also been studied by Francis et al. (2001). A simple explanation for the red colors is that these objects are heavily reddened. However, this model requires some extreme fine tuning so that Lyman- $\alpha$  can escape with relatively large EW while the I band flux is dominated by the reddened component.

An alternative explanation is that an older stellar population is present in the sample objects. This is illustrated by the solid lines in Figure 2 which show the resulting colors and equivalent widths obtained by combining young populations with age between 1 and 10 Myrs (top to bottom

on each line) with an older stellar population 1 Gyr in age. The mass ratio of the “old” to the young population is used to label the curves.

Both explanations require the underlying “hidden” population to greatly exceed the mass of the young population directly responsible for the Lyman- $\alpha$  emission. For a two population mix with an age of 1 Gyr for the oldest population, one needs “hidden” masses that are 4000 and 8000 times the young population mass in order to obtain B-I colors of 1.5 or 2, respectively. If the observed colors are due to dust, one needs a reddened component 10000 times more massive than the unreddened population. This factor has been calculated for the case of a screen of dust. Other dust geometries would increase extinction without increasing reddening and would lead to even larger factors. The minimum masses quoted above have been determined by considering a range from 100 Myr to 2 Gyr in age for the older population in the population mix model, and dust reddening values ranging from  $A_V$  of 1 through 10 for the dust reddening model. We have also found that our results do not depend critically on metallicity.

#### 4. Discussion and Conclusions

By using a custom medium band filter, we have detected a large number of bona fide Lyman- $\alpha$  emitters. A total of 31 blue candidates have been excluded by our [OII] rejection criteria. However, their inclusion would not have changed our conclusion that the majority of our candidates are red. On average the emitters have colors much redder than those expected for young, non-reddened, starbursts. Objects with similarly red colors would be hard to find in typical Lyman-break searches because such searches typically require a blue color longwards of the break. The red color of Lyman- $\alpha$  emitters at  $z \sim 2.4$  was noted also by Campos et al. (1999) who, however, did not attempt to model the effect. In order to account for the red colors one needs a large fraction of the stellar mass to be either old or highly reddened. Francis et al. (2001) reached a similar conclusion for the two red compact objects they found within a more extended Lyman- $\alpha$  nebula at  $z \simeq 2.38$ . Note that this conclusion (and the stellar masses derived below) would remain valid even if we were simply detecting Seyfert nuclei rather than star formation. We do not think that this is the case since, by assuming the Seyfert nuclei luminosity function at  $z=2.4$  to be the local one (e.g. Köhler et al. 1997) scaled up to match that of QSOs at  $z \simeq 2.3$  (Boyle et al. 2000), we still find that less than a dozen of our final sources would be expected to be an AGN.

If the observed colors are interpreted as due to dust reddening, the global star formation rate from this population would have to be enhanced by a factor 10000 or more, thus exceeding by two order of magnitudes the global peak star formation rate estimated by Madau et al. (1996). This makes it unlikely that reddening is the general explanation of the red colors in our sample objects.

If instead an old population is present, one can estimate its relative importance as follows. The minimum excess of old population is obtained for a 1 Gyr old population. For the young population an age of 5 Myrs is representative of the result (ages below about 10 Myrs are needed

to produce the observed EW). Assuming that the bursts are separated by no less than 10 Myrs, we obtain a maximum of 100 for the number of bursts that can have taken place. Since the mass of the old population exceeds that of the young population by much more than a factor 100, the old population must dominate the mass by at least a factor 10, implying that the star formation episodes that we are witnessing are neither the first nor the most important ones in the life of these galaxies. Indeed for a typical object in our sample, by using Bruzual & Charlot models and a Salpeter mass function between 0.1 and 125  $M_{\odot}$ , we derive from the Lyman- $\alpha$  flux that the mass of the unreddened young population is  $\sim 10^7 M_{\odot}$ , implying total stellar masses of  $\sim 10^{11} M_{\odot}$ . The number density of our sources is about 5 per cent that of  $L_{\star}$  galaxies or brighter and is compatible with that of EROs or elliptical galaxies as long as the duty cycle of accretion/star formation is high (50-100 per cent). These arguments suggest that these objects might have formed already most of their stars by  $z \simeq 2.4$  and therefore that they might be proto-elliptical galaxies (Spinrad et al. 1997, Stiavelli et al. 1999).

We thank S. Lilly and M. Fall for extensive discussions and constructive criticism, the anonymous referee for suggestions that helped improving the paper, M. Dickinson, R. Ellis and S. Djorgovski for useful comments and P. Madau for making available his intergalactic extinction curves. This project has been partially supported by the SNS in Pisa, the MURST of Italy and by the STScI DDRF grant 82241.

## REFERENCES

- Bertin, E., & Arnouts, S. 1996, A&AS, 117, 393
- Boyle, B. J., Shanks, T., Croom, S. M., Smith, R. J., Miller, L., Loaring, N., & Heymans, C. 2000, MNRAS, 317, 1014
- Bruzual, A. G., & Charlot, S. 1993, ApJ, 405, 538
- Burstein, D., & Heiles, C., 1982, AJ, 87, 1165
- Calzetti, D., Heckman, T. M. 1999 ApJ, 519, 27
- Campos, A., Yahil, A., Windhorst, R. A., Richards, E. A., Pascarelle, S., Impey, C., & Petry, C. 1999, ApJ, 511, L1
- Carollo, C. M., & Lilly, S. J., 2001, ApJ, 548, L153
- Charlot, S., & Fall, S. M. 1993, ApJ, 415, 580
- de Propris, R., Pritchet, C.J., Hartwick, F.D.A., Hickson, P., 1993, AJ, 105, 1243
- Francis, P. J., Williger, G. M., Collins, N. R., Palunas, P., Malumuth, E. M., Woodgate, B. E., Teplitz, H. I., Smette, A., Sutherland, R. S., Danks, A. C., Hill, R. S., Lindler, D., Kimble, R. A., Heap, S. A., Hutchings, J. B. 2001, ApJ, in press
- Giavalisco, M., Koratkar, A., & Calzetti, D. 1996, ApJ, 466, 831
- Jansen, R. A., Fabricant, D., Franx, M., & Caldwell, N. 2000, ApJS, 126, 331
- Kennicutt, R. C., Tamblyn, P., & Congdon, C. E. 1994, ApJ, 435, 22
- Kennicutt, R. 1998, in The Next-Generation Space Telescope Science Drivers and Technological Challenges, ed. J. P. Swings & B. Kaldeich-Schrmann (ESA SP-429; Noordwijk: ESA), 81
- Koehler, T., Groote, D., Reimers, D., & Wisotzki, L. 1997, A&A, 325, 502
- Kobulnicky, H. A. & Koo, D. C. 2000, ApJ, 545, 712
- Landolt, A. U. 1992, AJ, 104, 340
- Lilly, S. J., Le Fevre, O., Hammer, F., Crampton, D. 1996, ApJ, 460, 1
- McQuade, K., Calzetti, D., Kinney, A.L., 1995, ApJS, 97, 331
- Madau, P. 1995, ApJ, 441, 18
- Madau, P., Ferguson, H.C., Dickinson, M.E., Giavalisco, M., Steidel, C.C., Fruchter, A. 1996, MNRAS, 283, 1388



- Metcalfe, N., Shanks, T., Campos, A., McCracken, H.J., Fong, R., MNRAS, 323, 795
- Meurer, G.R., Heckman, T.M., Calzetti, D. 1999, ApJ, 521, 64
- Moorwood, A.F.M., van der Werf, P.P., Cuby, J. G., Oliva, E. 2000, A&A, 362, 9
- Oke, J. B., 1974, ApJS, 27, 21
- Pei, Y.C. & Fall, S.M. 1995, ApJ, 454, 69
- Pei, Y.C., Fall, S.M., Hauser, M.G. 1999, ApJ, 522, 604
- Pettini, M., Shapley, A.E., Steidel, C.C., Cuby, J.-G., Dickinson, M., Moorwood, A.F.M., Adelberger, K.L., Giavalisco, M., 2001, ApJ, 554, in press
- Schlegel, D. J. et al. 1998, ApJ, 500, 525
- Scarlata, C., Stiavelli, M., Lilly, S., Treu, T., Bertin, G., 2001, in preparation
- Spinrad, H., Dey, A., Stern, D., Dunlop, J., Peacock, J., Jimenez, R., Windhorst, R. 1997, ApJ, 484, 581
- Steidel, C. C., Giavalisco, M., Pettini, M., Dickinson, M., & Adelberger, K. L. 1996, ApJ, 462, L17
- Steidel, C. C., Adelberger, K. L., Dickinson, M., Giavalisco, M., Pettini, M., Kellogg, M. 1998, ApJ, 492, 428
- Steidel, C. C., Adelberger, K. L., Shapley, A. E., Pettini, M., Dickinson, M., & Giavalisco, M. 2000, ApJ, 532, 170
- Stiavelli, M. 1998, in The Next-Generation Space Telescope Science Drivers and Technological Challenges, ed. J. P. Swings & B. Kaldeich-Schrmann (ESA SP-429; Noordwijk: ESA), 71
- Stiavelli, M., Treu, T., Carollo, C. M., Rosati, P., Viezzer, R., Casertano, S., Dickinson, M., Ferguson, H., Fruchter, A., Madau, P., Martin, C., Teplitz, H. 1999, A&A, 343, L25
- Thompson, D., Djorgovski, S., Trauger, J., 1995, AJ, 110, 963
- Treu, T., Stiavelli, M. 1999, ApJ, 524, L27

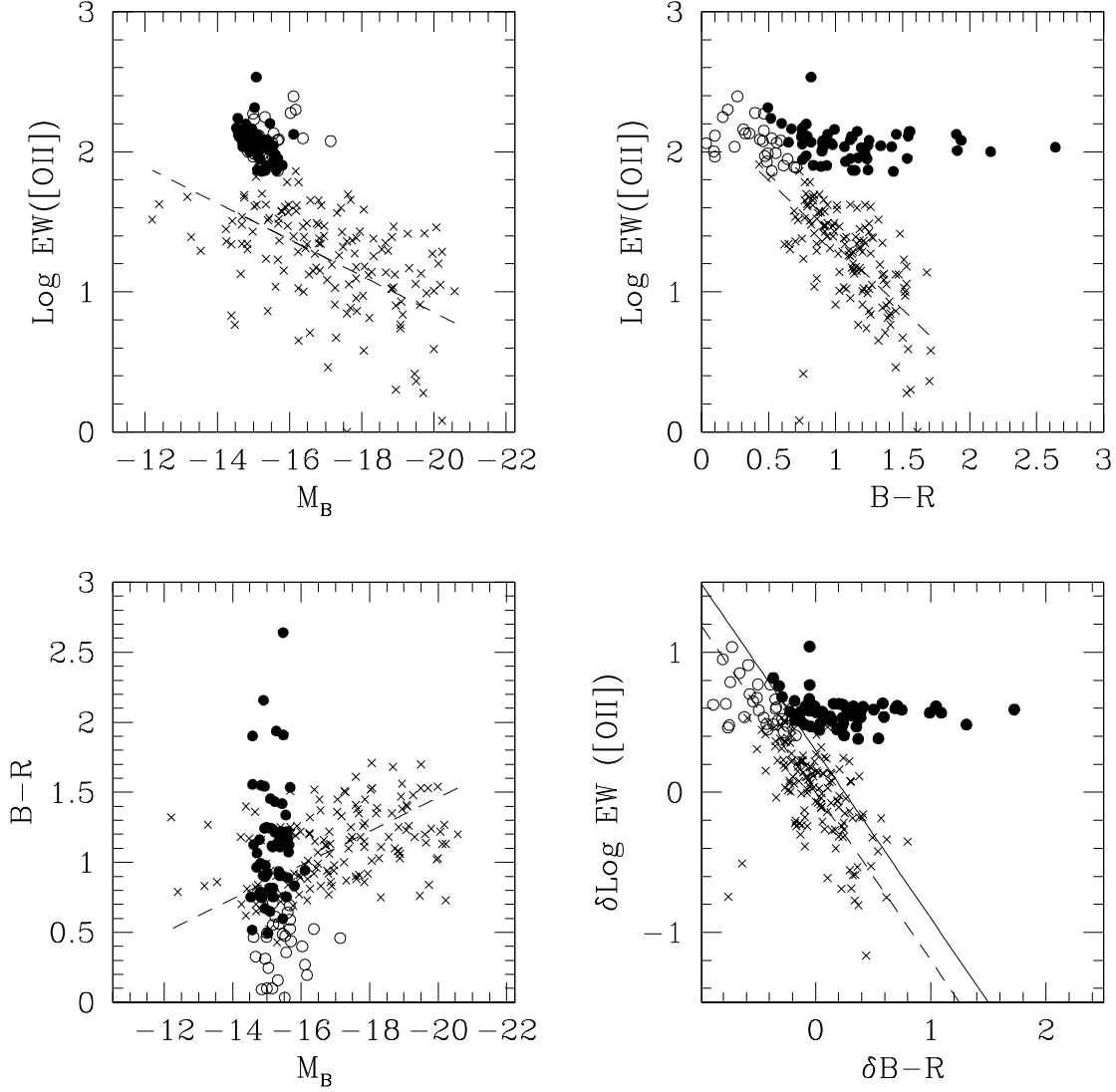


Fig. 1.— We plot various correlations for local [OII] emitters (Jansen et al. 2000, crosses) and for our candidates (open and filled circles) assuming all of our candidates are actually interlopers located at  $z \simeq 0.11$ . On the Log EW (observed) vs absolute magnitude plot (top left panel) the local [OII] emitters are on average brighter and with lower EW than our candidates. Similarly in the Log EW (observed) vs  $B-R$  color (top right panel) the local [OII] emitters are bluer than our candidates. The dashed lines are fits to the local [OII] emitters. The bottom left panel shows the color-magnitude relation for the local [OII] emitters and the lack of a correlation for our candidates. The bottom right panel shows a delta-delta plot where for each object we have used the EW vs  $M_B$  and  $B-R$  vs  $M_B$  fits to show the departures of EW and  $B-R$  color from the expected values on the basis of the observed absolute magnitude. This diagram is used by us to separate our bona fide Lyman- $\alpha$  emitters (filled circles, to the right of the solid line) from the possible [OII] contaminants (open circles, to the left of the solid line).

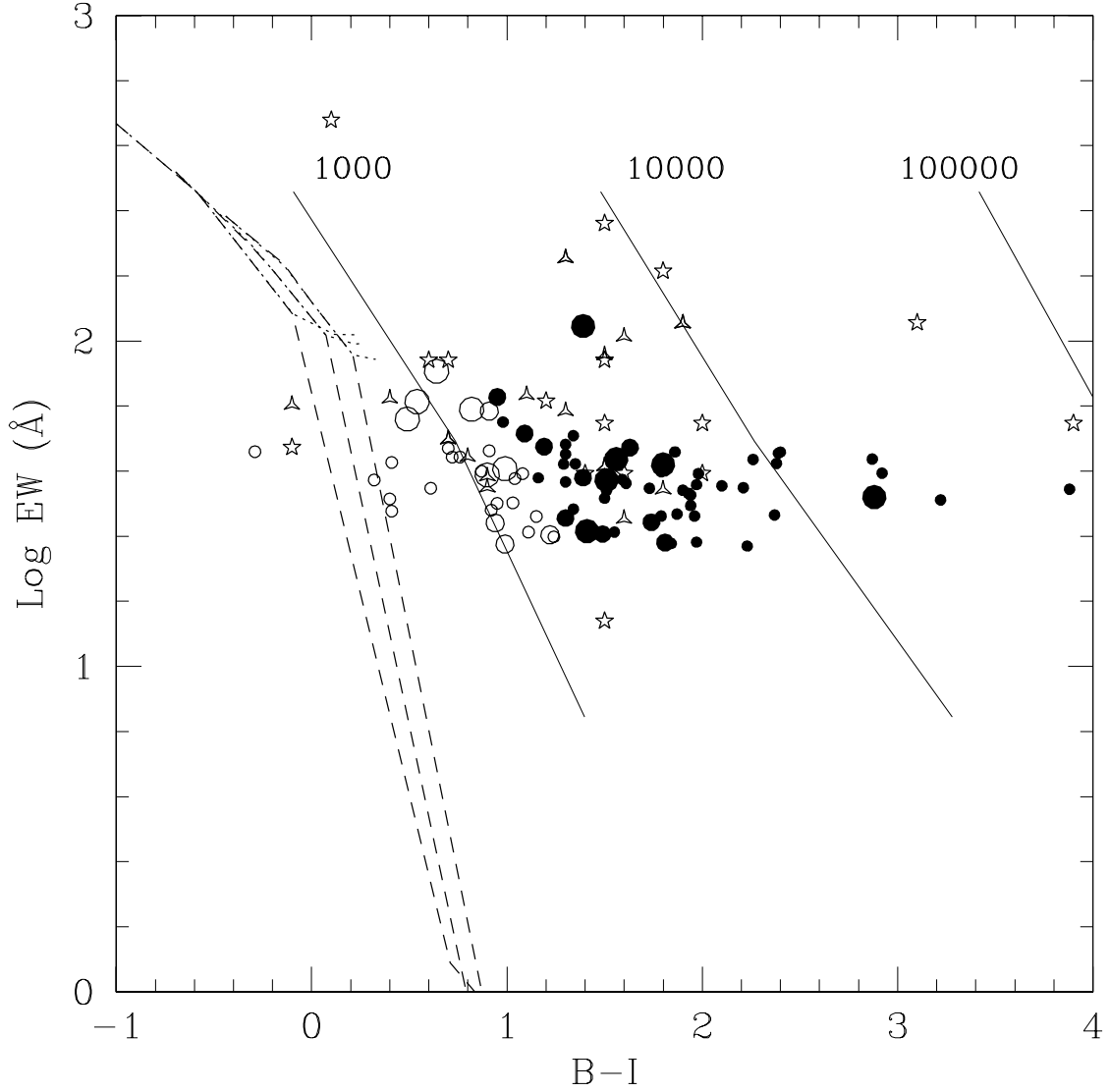


Fig. 2.— The Log EW (rest frame) vs the observed B-I color is plotted for our sample (filled circles). The symbol size identifies objects detected at a 5 (largest), 4 (intermediate), and 3- $\sigma$  (smallest) level. Possible low redshift contaminants ([OII] emitters) are plotted as open circles. Also shown are the objects from Pascarelle et al. 1998 for the cluster (open triangles) and the field (open stars). The dotted and dashed lines give the relation between EW and B-I color for continuous and single burst models, respectively, calculated using Bruzual & Charlot (BC96, with metallicity of 0.2  $Z_{\odot}$ , 0.4  $Z_{\odot}$  and  $Z_{\odot}$ ). The solid lines show the colors and equivalent widths obtained by combining young populations with age between 1 and 10 Myrs (top to bottom on each line) with an older stellar population 1 Gyr in age. The mass ratio of the old to the young population is used to label the curves. All the two component models have metallicity 0.4  $Z_{\odot}$ .